

COMBINING EXPERIMENTAL DATA AND NUMERICAL MODELING TO ANALYZE TRAIN-STRUCTURE INTERACTION ON THE HISTORIC SAN MICHELE BRIDGE (ITALY, 1889)

Lorenzo Ermolli¹, Michele Guerini¹, Charikleia D. Stoura^{2,3}, Rosalba Ferrari¹,
Vasilis K. Dertimanis², Eleni N. Chatzi², Egidio Rizzi¹

¹ Dipartimento di Ingegneria e Scienze Applicate, Università degli studi di Bergamo
viale G. Marconi 5, I-24044 Dalmine (BG), Italy
l.ermolli@studenti.unibg.it, michele.guerini@unibg.it, rosalba.ferrari@unibg.it, egidio.rizzi@unibg.it

² Department of Civil, Environmental and Geomatic Engineering, ETH Zürich
Stefano-Franscini-Platz 5, 8093 Zürich, Switzerland
charikleia.stoura@ibk.baug.ethz.ch, v.derti@ibk.baug.ethz.ch, chatzi@ibk.baug.ethz.ch

³ Department of Mechanical Engineering, Politecnico di Milano
via La Masa 1, 20156 Milan (MI), Italy
charikleia.stoura@polimi.it

Abstract. *As part of ongoing efforts to study and preserve the San Michele Bridge, a remarkable example of 19th-century iron architecture and a true symbol of Italian industrial archaeology, an experimental campaign was conducted on it in May 2024. Completed in 1889 by the Società Nazionale delle Officine di Savigliano (SNOS), the San Michele Bridge spans 266 meters across the Adda River, connecting the towns of Paderno d'Adda (Lecco bank) and Calusco d'Adda (Bergamo bank) in Lombardy, northern Italy. Its innovative design features a doubly built-in parabolic arch and an upper continuous beam, supporting both railway and road traffic. During the experimental campaign, accelerometers were deployed both on the bridge structure and on a crossing railway vehicle, allowing for the simultaneous collection of acceleration data from both systems, aiming at investigating the dynamic behavior of the bridge under vehicle-bridge interaction effects, which constitutes a significant excitation mechanism for the bridge structure. This study presents a preliminary dynamic analysis on the bridge that first models the railway vehicle crossings as moving loads through a finite element model of the bridge, enabling numerical simulations of the system's dynamic response. Then, it foresees a comparison of numerical predictions with experimental data, in order to refine the FEM model and gain insight into the dynamic interaction of the coupled vehicle-bridge system under operating conditions. This research is part of a broader initiative to establish a comprehensive Structural Health Monitoring (SHM) platform for the San Michele Bridge. Such a system would enhance long-term monitoring, facilitate early damage detection, and support the preservation and safety of this historic viaduct. The findings highlight the importance of integrating advanced experimental techniques with numerical modeling to safeguard valuable, historic infrastructure.*

Keywords: Railway bridge, FEM model, Moving load, Dynamic interaction, Modal updating.

1 INTRODUCTION

The San Michele Bridge was built during the 19th century to connect the provinces of Lecco and Bergamo, otherwise separated by the Adda River, between Paderno d'Adda (LC) and Calusco d'Adda (BG). This structure is a remarkable example of an arch bridge, consisting of a continuous box girder supported by nine bearings, four of which directly resting on the 150-meter-span arch. Given its historical and still present territorial significance the preservation of such iconic infrastructure is of paramount importance. To this end, the creation of a long-term Structural Health Monitoring (SHM) platform for the Paderno d'Adda Bridge was proposed in [5]. The project also aims to extend the knowledge acquired during this phase of the study on the San Michele Bridge to other similar infrastructures. The SHM platform to be developed will be based on a digital twin of the structure that may facilitate early damage detection, improve predictive maintenance, and most importantly contribute to the preservation of this significant historical structure.

As a starting point for the development of this project, an experimental campaign was conducted in May 2024 as a joint effort between research groups from the University of Bergamo and ETH Zurich, aiming at investigating the dynamic behaviour of the bridge under vehicle-structure interaction effects. The experimental campaign was carried out without closing the bridge to regular transit and taking advantage of the nighttime when train traffic is usually stopped and road traffic very limited. This permitted to have time and space to set up all the instrumentation. Acceleration data were recorded under both ambient and loaded conditions, the latter involving multiple crossings of a special railway convoy at various speeds. To simultaneously capture the dynamic response of the bridge and the convoy, a data acquisition system equipped with accelerometers was installed on both the bridge and the train.

The primary goal of the study here presented is to investigate the effect of a moving load on the structure by foreseeing a comparison among simulations carried out numerically with a dedicated FEM model of the structure with real data acquired during the experimental campaign. The adopted San Michele Bridge FEM model is based on that previously developed by the UniBG Research Group [5, 6] and adapted for the dynamic simulations of multiple moving loads [10, 18, 20], representing the convoy used during the experimental campaign. Due to the location of the sensors during the campaign, a part of the bridge structure rather than the entire bridge model is used to perform the aforementioned simulations. The subpart of interest includes the upper continuous beam of the bridge where the trains travel, within it. To simulate the effects of the supporting substructures (arch and piers), which do not form part of the substructure of interest, elastic boundary conditions are introduced, in the form of springs, to be calibrated.

This study is presented as follows: in Section 2 the experimental campaign is described, providing some information about the sensor positioning and the rail-vehicles used to perform dynamic tests on the structure. Following Section 3 presents the FEM model of the Paderno d'Adda Bridge, including the substructuring process, the initial guess procedure of the spring stiffnesses introduced at the level of the upper continuous beam, and lastly the moving load modelling of the train convoy. Then, Section 4 presents preliminary numerical results of dynamic simulations under moving loads. Lastly, Conclusions present the main findings of this study.

2 EXPERIMENTAL CAMPAIGN

In May 2024, an extensive experimental campaign was carried out during two overnight sessions, taking advantage of the usual suspension of train traffic. Acceleration response signals to ambient excitation, road traffic and dedicated rail-vehicle passage were collected, with the aim of gathering information on the structural behaviour under traffic conditions of road and train traffic and investigating the vehicle-bridge interaction in further analyses.

To acquire acceleration signals, 12 uniaxial seismic accelerometers *Model 731A, Wilcoxon* were installed on the bridge at the railway level inside the upper continuous beam, where rail-vehicles transited during controlled tests. Accelerations were measured in both transverse horizontal and vertical directions. Details about sensor positioning are illustrated in Figure 1. Some sensors were positioned at the level of the piers, while others were installed slightly offset from them, except for a couple of sensors placed at the key of the arch.

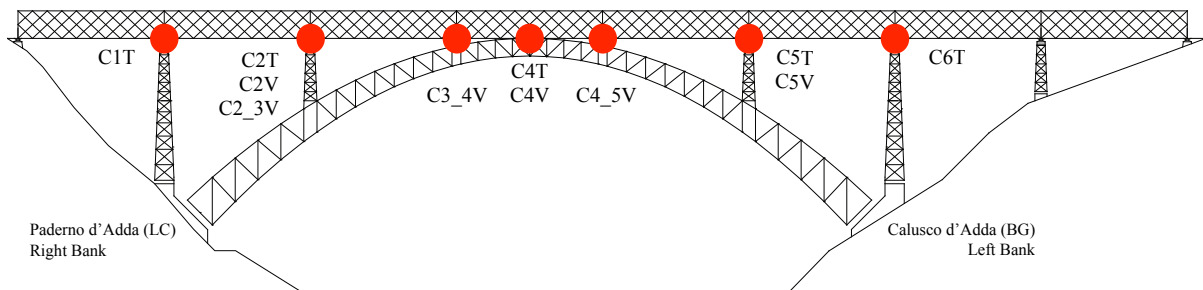


Figure 1: San Michele Bridge (1889), structure and sensor configuration adopted during the experimental campaign (May 2024). Solid red dots indicate sensor location, and labels report number of span and direction, namely “T” for Transverse horizontal direction and “V” for Vertical direction.

During the campaign, dynamic tests were performed with a dedicated rail-vehicle instrumented on the axles with monoaxial and triaxial accelerometers. The tests consisted in the controlled passage of the vehicles represented in Figure 2, at different speeds, moving directions, and configurations. In particular, two configurations were adopted: a locomotive only (a), and locomotive with a short convoy of two wagons (b).



(a) Locomotive



(b) Two-wagon convoy

Figure 2: Representation of the locomotive (a) and the two-wagon convoy (b) employed during the experimental campaign (May 2024).

These vehicles ran over the bridge from Paderno d'Adda to Calusco d'Adda and viceversa at different controlled speeds, ranging from 3 km/h to 15 km/h, and the structural response was registered with accelerometers positioned on both structure and vehicle.

For the purposes of this study, only the acceleration signals from structure-mounted sensors are considered, specifically from tests conducted with the locomotive and two-wagon convoy travelling from Paderno d'Adda to Calusco d'Adda.

3 BRIDGE FINITE ELEMENT MODEL

The initial idea was to numerically simulate the dynamic behavior of the structure under a moving load, designed to be as representative as possible of the rail-vehicle employed for the aforementioned dynamic tests.

To achieve this, the FEM model of the bridge, originally developed in MATLAB for static and limit analyses [5, 6] was employed. The model was created using Euler-Bernoulli beam elements, whose mechanical properties were derived directly from the original design drawings. The model was formulated in three dimensions and consisted in 5337 beam elements, 2216 nodes, and 13296 degrees of freedom (dofs). The global FEM model represented the entire structure, including the five piers, the doubly built-in parabolic arch and the upper continuous beam.

For the moving load simulations, only the 3D box-formed upper continuous beam was retained. To capture the influence of the substructure, translational springs were added in the transverse, horizontal, and vertical directions, with stiffness coefficient to be calibrated.

Finally, the damping matrix was defined using a Rayleigh damping model [3]. The two Rayleigh coefficients were determined by solving the system of equations corresponding to a damping ratio of 1% for the first two vibration modes of the structure.

3.1 Substructuring of the bridge

A substructuring approach was adopted to isolate the continuous box girder from the rest of the structure. This process required the implementation of translational springs in the numerical model, to reproduce the supporting conditions otherwise provided by the piers and the bridge arch.

The new boundary conditions were defined under the assumption that the main load-bearing element, i.e. the parabolic arch, primarily undergoes flexural deformations, in addition to axial effects. Instead, the piers mainly experience (limited) axial deformations in the vertical direction, with a contained flexural contribution in the transverse horizontal and longitudinal directions. A schematic 2D drawing of the substructuring process is shown in Figure 3 where boundary conditions were imposed on the 3D box-formed upper continuous beam substructure as a result of the removal of supporting structures.

Concerning the vertical direction for the four supports directly connected to the arch, the induced deformations are governed by the flexural response of the arch rather than by axial effects. For this reason, translational elastic springs are introduced only at the corresponding positions to account for the higher deformation. Specifically, starting from the Paderno d'Adda side (left side according to Figure 3), a couple of elastic springs is located at the second, third, fourth, and fifth bearings both downstream and upstream, as the substructured model is still 3D. All remaining supports, namely at the bridge extremities and at the bearings on the ground, are described by absolute rollers.

To avoid defining an excessive number of springs, the symmetry of the bridge is assumed

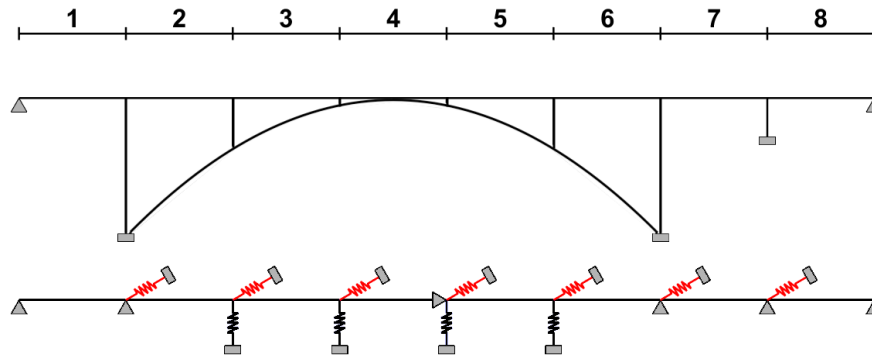


Figure 3: Planar schematic representation of the substructuring process applied to the bridge FEM model. While the beam substructure remains 3D and springs are applied on both sides of the bridge, only one side is illustrated here for clarity. Vertical springs are shown in black and transverse horizontal springs in red.

along the longitudinal direction and with respect to the keystone of the arch. Consequently, each couple has the same stiffness value, and the stiffness of the second couple of springs (between the second and third spans) is assumed equal to that of the fifth spring (between the fifth and sixth spans), while the stiffness of the third spring (between the third and fourth spans) is equal to that of the fourth spring (between the fourth and fifth spans), resulting in two stiffness values to be calibrated in the vertical direction.

In the transverse horizontal direction, the behaviour of the continuous box beam differs significantly. In this case, no symmetry axis was found other than the longitudinal one, resulting in seven distinct stiffness values.

Therefore, boundary conditions are applied exclusively to the edge beams on the lower deck of the box section, as the central beams do not rest on the piers.

The substructured FEM model of the box beam comprises 3,648 beam elements and 4,308 unconstrained dynamic DOFs, including 22 elastic springs defined at the boundaries with the eliminated substructures, of which 9 parameters must be calibrated. Although these values shall be refined through a modal updating procedure, it is essential to provide initial values that may best represent the actual boundary conditions.

To initialize the stiffness values of these springs, two distinct static scenarios are considered, each aimed at calibrating the stiffness of the springs in a specific direction. In both cases, initialization is performed by ensuring the equivalence of displacement values, assessed through static analyses, recorded under different loading scenarios.

For the vertical springs, the selected loading scenario corresponds to the self-weight of the entire structure. A static analysis of the entire structure is conducted, recording the vertical displacement values at the spring application points. The stiffness values are then adjusted until the displacements between the two models converge. The maximum percentage difference between the substructure's deformed shape and the entire bridge's deformed shape is approximately 1.63%. This static analysis additionally confirms that these points exhibited symmetrical behaviour, validating the initial modelling assumption.

To define initial values in the transverse horizontal direction, transverse forces of equal magnitude are applied at the spring locations. Similar to the calibration process in the vertical direction, the spring stiffness values are determined so that they ensure that the transverse displacements closely match those evaluated in the full-structure model. For this case, the maximum percentage difference between the substructure's deformed shape and the bridge's deformed shape is approximately 3.46%.

Stiffness values of the springs introduced in the upper continuous beam, extracted from the complete model, are reported in Table 1, where they are distinguished in transverse horizontal and vertical directions.

Bearing n. / Direction	1	2	3	4	5	6	7
Horizontal	23000	12000	2900	3100	4800	7500	34000
Vertical	-	74000	47000	47000	74000	-	-

Table 1: Stiffness values of the springs introduced in the substructure of the Paderno d'Adda Bridge (1889), to represent the effect of the structure under the box-formed upper continuous beam. Values are reported in kN/m.

Figures 4 and 5 illustrate the static deformed shapes of the system for the vertical and transverse horizontal direction spring calibrations, respectively. In each scenario, the deformation of the entire structure is shown first followed by that of the upper substructure only.

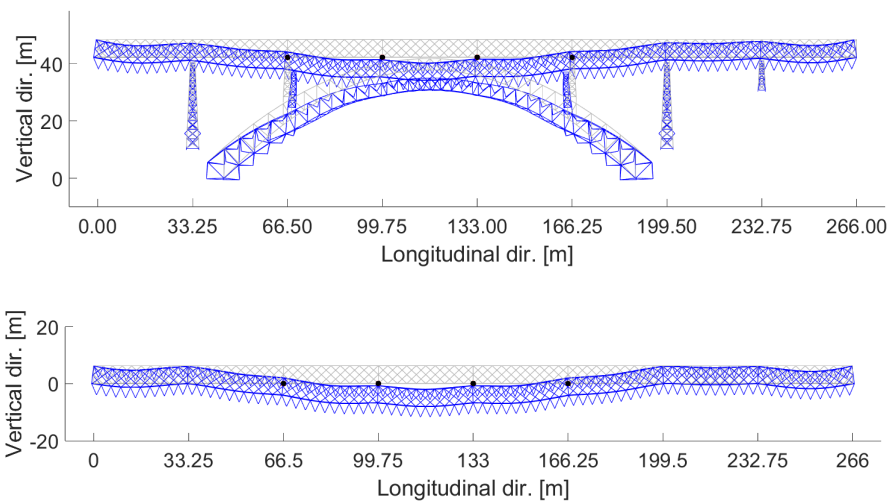


Figure 4: Deformations of full (up) and substructured (down) bridge models in the vertical-longitudinal two-dimensional plane. The deformed shape is shown in blue, the undeformed shape in grey, and the black circles indicate the positions of the vertical springs.

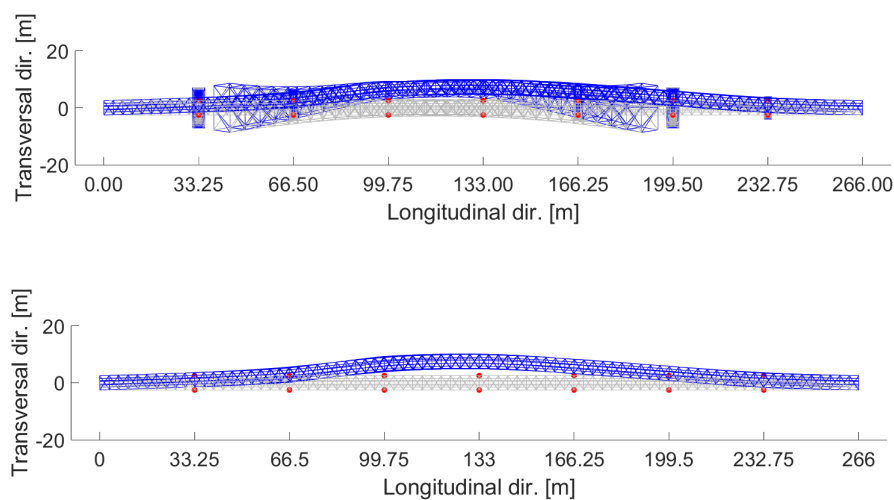


Figure 5: Deformations of full (up) and substructured (down) bridge models in the transverse-longitudinal two-dimensional plane. The deformed shape is shown in blue, the undeformed shape in grey, and the red circles indicate the positions of the transverse horizontal springs.

3.2 Modelling of the rail vehicle as moving loads on the FEM model of the beam

The test rail-vehicle represented by Figure 2 is simplified for the simulation as a sequence of moving loads acting on the rails. These loads were calibrated to reproduce as closely as possible the loading conditions (i.e. the weight of the wagons and locomotive axles) imposed during the experimental campaign. The simplified representation of the convoy is illustrated in Figure 6, where the load is represented by the red arrows and also the relative distance (in meters) between two consecutive axles. The weight of each axle is detailed in Table 2.

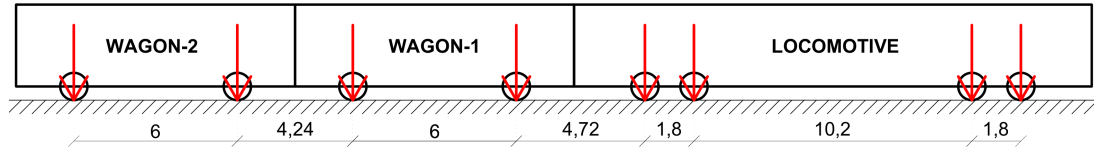


Figure 6: Convoy setup with a graphical representation of the axle spacings (in meters) for the railroad vehicle used during the experimental campaign.

Unit Type	Locomotive	Wagon-1	Wagon-2
1st axle	16.60	14.50	14.50
2nd axle	16.60	14.50	14.50
3rd axle	16.60		
4th axle	16.60		

Table 2: Axle loads [t] of the test convoy.

The sequence of moving loads is applied at the train wheel locations and its effect on the nodes of each beam FE is modelled with equivalent nodal forces varying at each time instant [10]. Consequently, each vertical moving load is distributed at the nodes of each beam via an equivalent vertical forces V_i and a bending moments W_i , as shown in Figure 7.

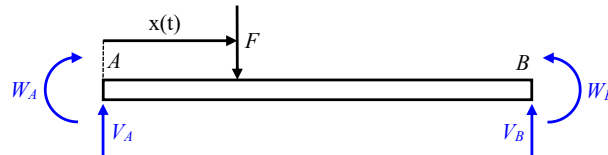


Figure 7: Equivalent nodal forces for a single beam element under a moving load of magnitude F at time instant t

The equivalent nodal forces on nodes A and B , for a single moving load of magnitude F , are determined as:

$$\begin{Bmatrix} V_A(t) \\ W_A(t) \\ V_B(t) \\ W_B(t) \end{Bmatrix} = F \begin{Bmatrix} 1 - \frac{3x^2}{l^2} + \frac{2x^3}{l^3} \\ x - \frac{2x^2}{l} + \frac{x^3}{l^2} \\ \frac{3x^2}{l^2} - \frac{2x^3}{l^3} \\ -\frac{x^2}{l} + \frac{x^3}{l^2} \end{Bmatrix} \quad (1)$$

According to Figure 6, a total of 16 moving loads must be set up to represent the forces transmitted to the bridge by the railroad vehicles: 8 on the left track and 8 on the right track.

Furthermore, it is assumed that the load moves from left to right (from Paderno d'Adda to Calusco d'Adda) at constant speed, as shown in Figure 8.

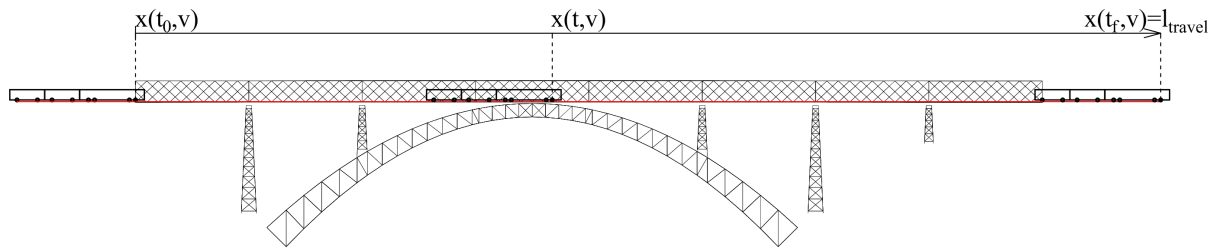


Figure 8: Modeling of the moving load on the San Michele Bridge. The Paderno d'Adda (LC) riverbank is shown on the left side, while the Calusco d'Adda (BG) riverbank, with the additional intermediate pier, is on the right side.

Eventually, the (linear) dynamic equations of motion for the discrete structural model are defined as follows:

$$\mathbf{M}\ddot{\mathbf{x}} + \mathbf{C}\dot{\mathbf{x}} + \mathbf{K}\mathbf{x} = \mathbf{F}(t) \quad (2)$$

The numerical integration of the second-order differential equations, Eq. (2), is computed by a classical Newmark method implementation with the average acceleration scheme. The numerical simulation starts when the first convoy axle enters the upper continuous beam and ends when the last axle exits the structure.

4 DYNAMIC SIMULATIONS OF THE TRAIN CONVOY

Several simulations were carried out with the aforementioned FEM model of the box-formed upper continuous beam of the Paderno d'Adda Bridge subjected to moving loads, testing different traversing speeds and configurations. In particular, in this section, the dynamic response in terms of displacement, velocity, and acceleration is presented for the load configuration in Figure 6, transiting at $v = 6 \text{ km/h} = 1.667 \text{ m/s}$ and at $v = 15 \text{ km/h} = 4.167 \text{ m/s}$. The time step size has been selected by the following relation:

$$\Delta t = \frac{h/v}{n} \quad (3)$$

where $h = 3.325 \text{ m}$ represents the length of the rail FEs where the load is applied, v is the speed of the convoy in m/s, and n is the number of steps taken by the moving load to travel along the entire length of the finite element. Adopting $n = 1000$ steps, the two time steps for the two speeds have corresponding size equal to 0.002 s and 0.000798 s .

The numerical results are represented in Figure 9 as time histories of displacement, velocity, and acceleration of the node located at the midpoint of the 4-th span, in correspondence of the key of the arch, at the level of the railway.

The preliminary results show that, although the train speed increases from 6 km/h to 15 km/h , which still represents a contained speeding condition, the displacement exhibits only a minor variation, whereas the velocity at the observed node rises by a factor of about three (notice the different scales in Figs. 9(c) and 9(d)). However, these initial results in terms of displacement and velocity cannot be experimentally validated, since no corresponding measurements were collected during the experimental campaign. Instead, accelerations from structure-mounted sensors shall be used in future studies to assess the quality of the present FEM simulations.

The effects of speed variation are instead more evident in the acceleration responses (notice again the different scales in Figs. 9(e) and 9(f)), as the node registers a maximum acceleration almost one order of magnitude larger, from about 1.5 mm/s^2 to 10 mm/s^2 when the speed increases from 6 km/h to 15 km/h .

However, these preliminary results seem to show discrepancies with higher acceleration responses recorded during the experimental campaign, suggesting that further modelling refinement shall be needed. As part of ongoing efforts, the first steps will involve also a dynamic calibration of the springs and updating the FEM model based on experimental responses and extracted modal properties [9]. Subsequent studies will focus on a deeper investigation of wheel-rail interaction to better capture its effect on the bridge's dynamic behaviour, also taking advantage of train-recorded signals.

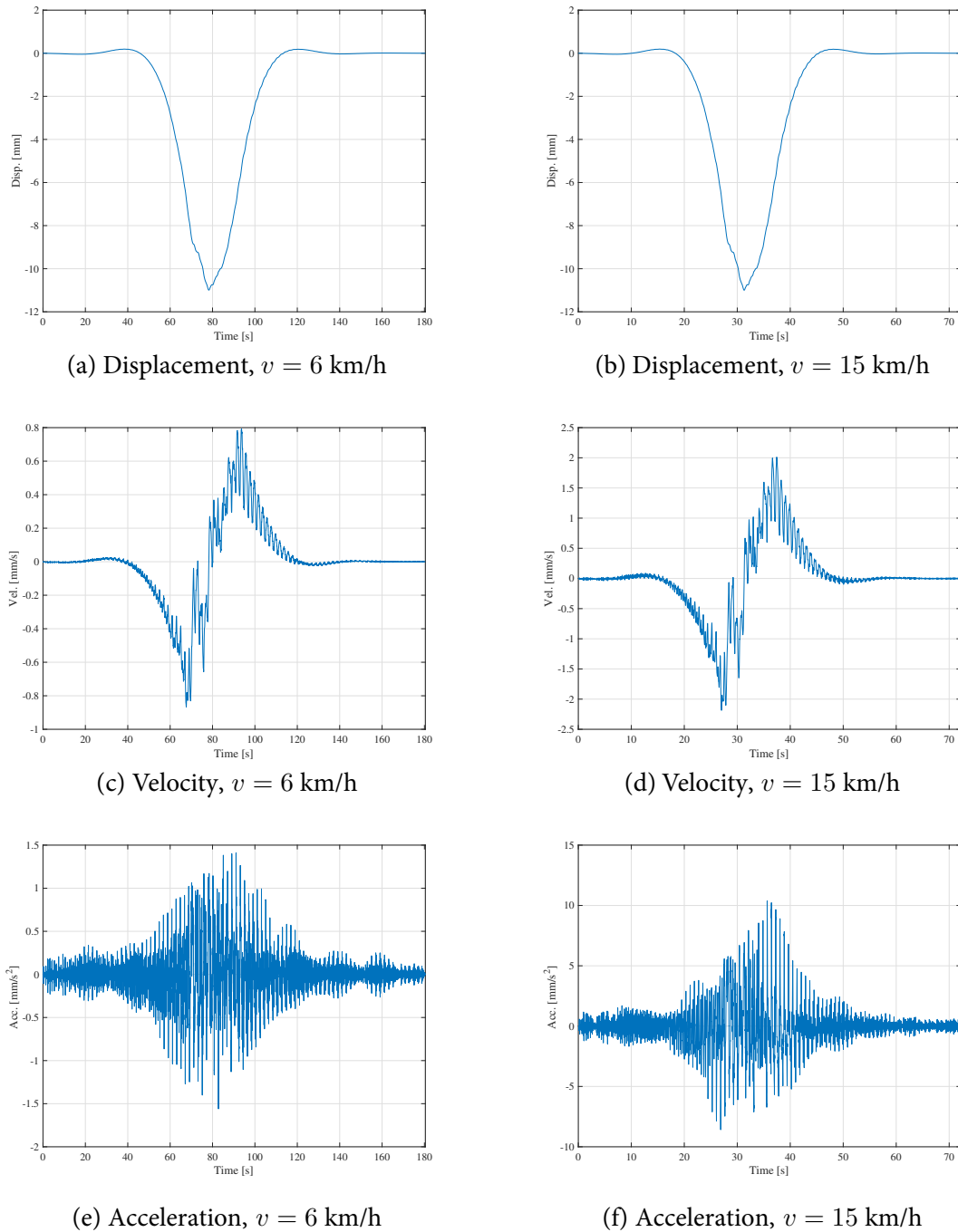


Figure 9: Displacement, velocity, and acceleration responses of the node located at the midpoint of the 4-th span at the key of the arch, when the moving loads transit at $v = 6$ km/h and $v = 15$ km/h.

5 CONCLUSIONS

The initial phase of a broader project devoted to the development of a SHM platform for San Michele Bridge (1889) provided insights into the dynamic behaviour of the infrastructure under ambient, road, and rail excitations. The experimental campaign conducted in May 2024, with sensors installed on both the structure and the test vehicles, provided an exhaustive dataset of structural responses for further analyses and model updating, to be post-processed.

This work reported first numerical simulations carried out within a modelling numerical framework. A FEM model of the structure was developed, based on a previous static model. Other elements, including a lumped mass matrix and Rayleigh damping, were introduced to enable dynamic analyses.

The FEM model was further substructured to retain only the 3D box-formed upper continuous beam, where the rail vehicles transit, within it. To account for the effects of the arch and piers, four vertical springs and seven transverse horizontal springs were added, on each side of the upper continuous beam. The linear dynamic equations of motion for a discrete structural model were solved numerically with the Newmark method.

The simulations highlighted interesting results, about displacement, velocity, and acceleration responses, accelerations likely looking underestimated, by the present modelling assumptions, with experimentally recorded ones. This may suggest possible improvements of the model, to better predict the dynamic behaviour of the Paderno d'Adda Bridge under moving problems. A detailed comparison between numerical and experimental responses shall be investigated in the future.

However, the present analysis proved the importance of including an algorithmic spring stiffness calibration and accounting for wheel-rail interaction. Ultimately, all these efforts shall support the development of a global Digital Twin of the San Michele Bridge (1889) designed to reproduce the bridge's real dynamic behaviour, providing an accurate digital representation of the real structure.

ACKNOWLEDGMENTS

The research conducted at the University of Bergamo was supported by the Italian Ministry of University and Research, through funding under the PRIN 2022 program and "Fondi di Ricerca d'Ateneo ex 60%". RFI, the bridge owner, is gratefully acknowledged for interaction and accessibility to the bridge. The third author would also like to acknowledge the Marie Skłodowska-Curie Actions (MSCA) program under the OMoRail project, Grant ID: 101104968.

REFERENCES

- [1] J.S. Bendat, A.G. Piersol *Random Data: Analysis and Measurement Procedures, 4th Edition*. Wiley, 2010.
- [2] R. Brincker, L. Zhang, P. Andersen, Modal identification from ambient responses using frequency domain decomposition. Society for Experimental Mechanics eds. *18th International Modal Analysis Conference (IMAC)*, San Antonio, Texas, USA, February 7-10, 2000.
- [3] A.K. Chopra, *Dynamics of Structures - Theory and Applications to Earthquake Engineering*, 4th Edition. Prentice Hall, 2011.

- [4] R.D. Cook, D.S. Malkus, M.E. Plesha, R.J. Witt, *Concepts and applications of finite element analysis, 4th Edition*, John Wiley & Sons, Inc., 2001.
- [5] R. Ferrari, E. Rizzi, M.S. Brioschi, V. Dertimanis, Design of an effective structural health monitoring platform for Paderno d'Adda Bridge (1889). *Reconstruction and Restoration of Architectural Heritage 2021*, S. Sementsov, A. Leontyev, S. Huerta eds., CRC Press, London, 210–215, 2021. DOI: 10.1201/9781003136804-41.
- [6] R. Ferrari, G. Cocchetti, E. Rizzi, Reference structural investigation on a 19th-century arch iron bridge loyal to design-stage conditions. *International Journal of Architectural Heritage*, **14**(10), 1425–1455, 2020. DOI:10.1080/15583058.2019.1613453.
- [7] R. Ferrari, D. Froio, E. Rizzi, C. Gentile, E.N. Chatzi Model updating of a historic concrete bridge by sensitivity- and global optimization-based Latin Hypercube Sampling, *Engineering Structures*, **179**(2019), 139–160, 2019. DOI: 10.1016/j.engstruct.2018.08.004.
- [8] C. Gentile, A. Saisi, Dynamic monitoring of the Paderno iron arch bridge (1889). B. Chen, J. Wei eds. *6th International Conference on Arch Bridges (ARCH'10)*, Fuzhou, China, October 11-13, 2010. Available at: <https://hdl.handle.net/11311/569851>.
- [9] M. Guerini, L. Ermolli, C.D. Stoura, R. Ferrari, V.K. Dertimanis, E.N. Chatzi, E. Rizzi, Modal dynamic identification of historic San Michele bridge (Italy, 1889). In Proceedings of *COMPdyn 2025 - 10th International Conference on Computational Methods in Structural Dynamics and Earthquake Engineering*, Rhodes, Greece, June 15-18, 2025, ID 26049. <https://2025.compdyn.org/proceedings>.
- [10] S.S. Law, J.Q. Bu, X.Q. Zhu, S.L. Chan, Vehicle axle loads identification using finite element method, *Engineering Structures*, **26**(8), 1143–1153, 2004. DOI: 10.1016/j.engstruct.2004.03.017.
- [11] F. Pioldi, R. Ferrari, E. Rizzi, Seismic FDD modal identification and monitoring of building properties from real strong-motion structural response signals. *Structural Control and Health Monitoring*, **24**(11), 1–20, 2017. DOI: 10.1002/stc.1982.
- [12] F. Pioldi, R. Ferrari, E. Rizzi, Earthquake structural modal estimates of multistorey frames by a refined Frequency Domain Decomposition algorithm. *Journal of Vibration and Control*, **23**(13), 2037–2063, 2015. DOI: 10.1177/1077546315608557.
- [13] F. Pioldi, R. Ferrari, E. Rizzi, Output-only modal dynamic identification of frames by a refined FDD algorithm at seismic input and high damping. *Mechanical Systems and Signal Processing*, **68–69**(2016), 265–291, 2016. DOI: 10.1016/j.ymssp.2015.07.004.
- [14] C.D. Stoura, E.G. Dimitrakopoulos EG, MDOF extension of the Modified Bridge System method for vehicle-bridge interaction. *Nonlinear Dynamics*, **102**(4), 2103–2123, 2020. DOI: 10.1007/s11071-020-06022-6.
- [15] C.D. Stoura, E.G. Dimitrakopoulos, A Modified Bridge System method to characterize and decouple vehicle-bridge interaction. *Acta Mechanica* **231**(9), 3825–3845, 2020. DOI: 10.1007/s00707-020-02699-3.

- [16] C.D. Stoura, E.G. Dimitrakopoulos, Additional damping effect on bridges because of vehicle-bridge interaction. *Journal of Sound and Vibration* **476**(2020), 115294, 2020. DOI: 10.1016/j.jsv.2020.115294.
- [17] C.D. Stoura, V.K. Dertimanis, E.N. Chatzi, Identification of railway bridge modal properties via acceleration data from traversing trains. R. Platz, G. Flynn, K. Neal, S. Ouellette eds. *42nd IMAC, A Conference and Exposition on Structural Dynamics*, Orlando, Florida, USA, January 29 - February 1, 2024. DOI: 10.1007/978-3-031-68893-5_12.
- [18] D. Froio, L. Verzeroli, R. Ferrari, E. Rizzi, On the numerical modelization of moving load beam problems by a dedicated parallel computing FEM implementation, *Archives of Computational Methods in Engineering*, **28**(4), 2253–2314, 2021.
- [19] S. Weng, Y. Xia, Y.L. Xu, H.P. Zhu, Substructure based approach to finite element model updating, *Computers and Structures*, **89**(9-10), 772–782, 2011. DOI: 10.1016/j.compstruc.2011.02.004.
- [20] Y.B. Yang, J.D. Yau, Y.S. Wu, *Vehicle-Bridge Interaction Dynamics: with Applications to High-Speed Railways*. World Scientific 2004.